Boundary condition independence of molecular dynamics simulations of planar elongational flow

Federico Frascoli,[1] B. D. Todd,[1,*] and Debra J. Searles[2,†]

[1]*Centre for Molecular Simulation, Swinburne University of Technology, P.O. Box 218, Hawthorn, Victoria 3122, Australia*
[2]*Nanoscale Science and Technology Centre, School of Biomolecular and Physical Sciences, Griffith University,*
Brisbane, QLD 4111, Australia

The simulation of liquid systems in a nonequilibrium steady state under planar elongational flow (PEF) for indefinite time is possible only with the use of the so-called Kraynik-Reinelt (KR) periodic boundary conditions (PBCs) on the simulation cell. These conditions admit a vast range of implementation parameters, which regulate how the unit lattice is deformed under elongation and periodically remapped onto itself. Clearly, nonequilibrium properties of homogeneous systems in a steady state have to be independent of the boundary conditions imposed on the unit cell. In order to confirm the independence of measurable properties of a system under PEF from the particular set of periodic boundary conditions, we compute the Lyapunov spectra, apply the conjugate pairing rule, and carefully analyze the so-called unpaired exponents for an atomic fluid of various sizes and state points. We further compute the elongational viscosity for various implementations of boundary conditions. All our results confirm the independence from KR PBCs for the dynamics of phase-space trajectories and for the transport coefficients.

I. INTRODUCTION

The chaotic properties of atomic liquid systems in a nonequilibrium steady state have been extensively studied in the last two decades [1–4]. The Lyapunov spectra for different field-driven systems out of equilibrium have been computed, and probably the most significant development is the establishment of a fundamental link between Lyapunov exponents and transport coefficients [4,5]. It is also noticeable that a growing interest in the Lyapunov modes of simple systems has developed in the last few years [6], showing that this field still presents us with the promise of providing valuable insights into fluid behavior.

The Sllod algorithm (so named because of its close relationship to the Dolls tensor algorithm) for planar elongation flow (PEF) [7] is a nonequilibrium molecular dynamics (NEMD) technique [3] and has some features that have important consequences on its chaotic properties. First of all, PEF adiabatic (i.e., unthermostatted) equations of motion are Hamiltonian. Second, the simulation of PEF systems requires the use of the so-called Kraynik-Reinelt (KR) periodic boundary conditions (PBCs) on the unit lattice [8], which are equivalent to carrying out the chaotic Arnold cat map [9,10]. Finally, Lyapunov spectra of PEF systems satisfy the so-called conjugate pairing rule (CPR) [11], which implies an equal sum for all Lyapunov pairs in the spectrum, formed by coupling the highest exponent with the lowest, the second highest with the second lowest, and so on. Generally speaking, it is also notable that the dynamics of PEF systems closely resembles that of some well-known discrete chaotic maps such as the Baker or Ikeda maps [12], as they all share the same "stretching and folding" type of behavior.

It is important to realize that the KR PBCs are essential for the simulation of this type of system: they are the only

known means that allow for these explicitly time-dependent simulations to run for an indefinite time [7,13,14] via a periodic remapping of the elongated unit cell onto itself. One fundamental aspect is that these PBCs can have different initial implementation parameters, which lead to different evolutions of the unit lattice under elongation. In fact, PEF simulations start (see Fig. 1) with the unit lattice rotated at an initial angle θ_0 with respect to the x axis and the magnitude of the deformation of the cell is described by the so-called Hencky strain ε_P [13], related to the lattice period τ_P (i.e., $\varepsilon_P = \dot{\varepsilon}\tau_P$, where $\dot{\varepsilon}$ is the reduced elongation rate defined in the next section). The values of these parameters can be inferred either from geometrical considerations on the unit lattice [8] or, in a more concise and elegant way, using the equivalence between the KR PBCs and the Arnold cat map [10].

The majority of the simulations reported in the literature have been conducted using only one particular set of initial conditions $(\theta_0, \varepsilon_P, \tau_P)$—namely, where the unit cell is initially rotated at an angle $\theta_0 = 31.72°$ and subject to a reduced Hencky strain $\varepsilon_P = 0.962$. To our knowledge, no systematic study of the independence of the physical properties, such as
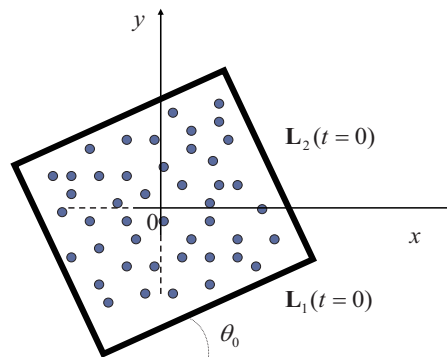

FIG. 1. (Color online) One of the possible initial positions of the unit lattice at the start of the simulation.

*Electronic address: btodd@swin.edu.au
†Electronic address: D.Bernhardt@griffith.edu.au

the transport coefficients, from these initial conditions has ever been attempted.

Even though any valid choice for $(\theta_0, \varepsilon_P, \tau_P)$ according to Refs. [8,10] ensures "reproducibility"—i.e., the spatial and temporal periodicity of the cell—and "compatibility," so that there is no violation of the minimum image convention throughout the simulation, different conditions do imply different evolutions for the lattice. Consequently, it is not excluded *a priori* that possible incompatible results for different parameters can arise, affecting phase-space trajectories or transport coefficients.

In relation to this, we recently suggested it might be possible to find any imprint of the KR boundary conditions in the dynamical properties of a PEF system by examining the Lyapunov spectra [11]. If the spectra depend upon the choice of the parameters of the KR scheme, then the physical properties of the system must likewise depend upon the way the sample within the unit cell is represented, in contrast with the fact that the fluid is homogeneous in time and space.

To investigate this, an analysis of Lyapunov spectra at different state points and with different initial conditions for simple atomic systems is carried out. The theory, algorithms, and results are presented in Sec. II. At first, systems with a large number of particles, N, are considered, giving evidence that the phase-space dynamics is invariant for different $(\theta_0, \varepsilon_P, \tau_P)$. Second, the case of a dilute $N=8$ particle system is discussed, showing that also in the low-size limit no PBC-related effect is present.

Finally, Sec. III contains some remarks on the relation between the Lyapunov exponents and the transport coefficients. This demonstrates the invariance of the latter with different initial conditions, assuring the validity and the reliability of the Sllod algorithm for PEF in combination with the KR procedure.

II. THEORY, DETAILS, AND RESULTS OF SIMULATIONS

To investigate the possible effects of different KR conditions on the dynamical properties of systems under PEF, we simulate samples of pointlike particle systems with the Sllod algorithm and maintain a constant-temperature nonequilibrium steady state with the use of the Gaussian isokinetic thermostat [3].

The particles interact via the Weeks-Chandler-Andersen (WCA) potential [15], which is a truncated and shifted version of the Lennard-Jones potential:

$$\phi(r_{ij}) = \begin{cases} 4\varepsilon\left[\left(\dfrac{\sigma}{r_{ij}}\right)^{12} - \left(\dfrac{\sigma}{r_{ij}}\right)^{6}\right] + \phi_c & \text{for } r_{ij} < r_c \\ 0 & \text{for } r_{ij} > r_c, \end{cases}$$

(1)

with $r_{ij} = |\mathbf{q}_i - \mathbf{q}_j|$, where $\mathbf{q}_i$ is the laboratory position vector of particle i, ε is the well depth, and σ is the value at which the Lennard-Jones potential is zero. ϕ_c is the value of the unshifted potential at the cutoff distance $r_c = 2^{1/6}\sigma$, so that the WCA potential is continuous. In the following we use reduced units, set all the masses of the particles m_i to be equal to m, and impose $m = \sigma = \varepsilon = 1$ for convenience.

The thermostatted equations of motion for the Sllod algorithm for a system of simple atoms under PEF, with expansion in the x direction and contraction in the y direction [7], are

$$\dot{\mathbf{q}}_i = \mathbf{p}_i + \dot{\varepsilon}(\mathbf{i}x_i - \mathbf{j}y_i),$$

$$\dot{\mathbf{p}}_i = \mathbf{F}_i - \dot{\varepsilon}(\mathbf{i}p_{xi} - \mathbf{j}p_{yi}) - \alpha\mathbf{p}_i,$$

(2)

where $\mathbf{p}_i$ is the peculiar momentum, or the momentum taken with respect to the streaming velocity $\mathbf{u}$, of the particle i, $\mathbf{i}$ and $\mathbf{j}$ are the unit vectors in the x and y directions, respectively, and $\dot{\varepsilon} = \frac{\partial u_x}{\partial x} = -\frac{\partial u_y}{\partial y}$ is the elongation rate. As the particle masses are defined to be unity, they are omitted from the equation. The Gaussian thermostat multiplier α has the form

$$\alpha = \frac{\displaystyle\sum_{i=1}^{N} \mathbf{F}_i \cdot \mathbf{p}_i - \dot{\varepsilon}(p_{xi}^2 - p_{yi}^2)}{\displaystyle\sum_{i=1}^{N} \mathbf{p}_i \cdot \mathbf{p}_i}.$$

(3)

To preserve homogeneity and eliminate surface effects, the use of "deforming-brick" PBCs is assumed [13]. They are essential to treat the fluid as a bulk, eliminating surface effects, and simulate the steady state in a consistent way. Because of them, the system, whose adiabatic equations [i.e., Eqs. (2) without the thermostat term $\alpha\mathbf{p}_i$] are Hamiltonian, is nonautonomous [16]. Also, a rezeroing of the y component of the total momentum at each time step is necessary to prevent an exponential growth of round-off errors, which are due only to the finite precision numerics and do not have any physical meaning. This procedure has no effect on any thermodynamically meaningful property of the system [17].

Lyapunov exponents measure the average rate of separation of two nearby phase-space trajectories. As there is one exponent for each degree of freedom in the system, the computation of the spectrum of Lyapunov exponents is performed with the well-established algorithm by Benettin *et al.* [18]. In short, consider a phase-space vector $\mathbf{\Gamma}_1(t) = [\mathbf{q}(t), \mathbf{p}(t)]^T$ and a displacement vector $\delta\mathbf{\Gamma}_n(t) = \mathbf{\Gamma}_1(t) - \mathbf{\Gamma}_n(t)$ whose evolution can be expressed to first order by $\dot{\delta\mathbf{\Gamma}}(t) = \mathbf{T}(t)\delta\mathbf{\Gamma}(t)$, where $\mathbf{T}$ is the stability matrix or the Jacobian of the equations of motion (2). We can then define a set of orthogonal vectors $\delta\mathbf{\Gamma}_n^c$, such that $\delta\mathbf{\Gamma}_n^c \cdot \delta\mathbf{\Gamma}_m^c = 0$ for all $m < n$, and consider the evolution of the set of vectors $\mathbf{\Gamma}_n^c(t) = \mathbf{\Gamma}(t) + \delta\mathbf{\Gamma}_n^c$. It can be shown that the set of Lyapunov exponents is then given by

$$\lambda_n = \lim_{t\to\infty} \lim_{\delta\mathbf{\Gamma}_n^c \to 0} \frac{1}{t} \ln\left(\frac{|\delta\mathbf{\Gamma}_n^c(t)|}{|\delta\mathbf{\Gamma}_n^c(0)|}\right).$$

(4)

The first sample of systems under analysis is made of two 2-dimensional large collections of particles ($N=512$ and $N=1058$ atoms) with reduced density $\rho=0.4$ and reduced temperature $T=1.0$ and subject to elongation rates $\dot{\varepsilon}=0.5$ and $\dot{\varepsilon}=1.0$. The size and the density allow for the implementation of various initial KR parameters which do not violate the minimum allowable lattice spacing. As the system size is decreased or the density is increased, the number of allowed

TABLE I. Initial conditions for the samples in this study: θ_0 is the initial angle of rotation for the unit lattice, ε_P is the Hencky strain, and m_i are the coefficients of the Arnold cat map associated with the KR PBCs.

Initial condition	θ_0	ε_P	m_1	m_2	m_3
1	13.28	2.887	17	−4	1
2	16.85	2.389	10	−3	1
3	21.14	2.704	13	−5	2
4	22.50	1.762	5	−2	1
5	31.72	0.962	2	−1	1
6	35.17	2.704	10	−7	5
7	31.72	1.925	5	−3	2
8	31.72	2.887	13	−8	5

$(\theta_0, \varepsilon_P, \tau_P)$ combinations decreases dramatically.

The connection between the KR PBCs and the Arnold cat map is explained in detail in [10]. We briefly recall only some useful results. If the 2×2 cat map matrix $\mathbf{M}$, where m_i are integer coefficients, is given by

$$\mathbf{M} = \begin{pmatrix} m_1 & m_2 \\ m_2 & m_3 \end{pmatrix},$$

then the eigenvalues are

$$\lambda_{1,2} = \frac{(m_1 + m_3) \pm \sqrt{(m_1 + m_3)^2 - 4}}{2}$$

and the Hencky strain ε_P is equal to $\ln(\lambda_{max})$, where λ_{max} is the maximum eigenvalue. If $\mathbf{e}_{max}$ is the eigenvector of $\mathbf{M}$ associated with λ_{max} and is aligned with the direction of maximum growth of the unit lattice under elongation [8], then the initial angle that the cell forms with the x axis is simply

$$\theta_0 = \cos^{-1}\left(\frac{1}{\|\mathbf{e}_{max}\|}\right). \tag{5}$$

As the Arnold cat map is area preserving—i.e., $\det(\mathbf{M}) = 1$—the coefficients are bounded by the relation $m_1 m_3 - m_2^2 = 1$.

The set of chosen initial conditions for our large N model is summarized in Table I. Besides the comparisons that can be done among different initial angles θ_0, there are also conditions with the same initial angle, different Hencky strain, and vice versa, so that any possible sensitivity of the model is under scrutiny. In fact, at equal elongation rates, the higher the Hencky strain, the longer the period and the larger the deformation of the cell. It is therefore reasonable to look at the effect that a different ε_P can have on cells that start at the same initial angle θ_0.

For each of these conditions, a fourth-order Gear predictor-corrector integrator is used, with a time step $\Delta t = 10^{-3}$ for a total simulation time of $t = 4000$ for $N = 512$ particles and $t = 1000$ for $N = 1058$. Every condition is sampled via three independent runs starting from a fcc lattice, where for each run the initial momenta are chosen randomly.

Results for the first six positive Lyapunov exponents are shown in Figs. 2–4. In Fig. 2, the value of the exponents is plotted according to the initial angle of rotation θ_0 for conditions 1–6 in Table I, where λ_1 is the maximum exponent, λ_2 is the second highest, and so on. All the values of appropriate exponents fall within each others' uncertainty, given as twice the standard error of the mean. Also, no pattern that can reveal any dependence from the angle is present, as values align around the mean without a preferred order.

In Fig. 3, the exponents for conditions 5, 7, and 8 are plotted. In this case, the angle is the same and the systems are subject to three different Hencky strains. No dependence of ε_P is observed in the exponents, even though ε_P for conditions 7 and 8 is, respectively, 2 and 3 times the ε_P for condition 5.
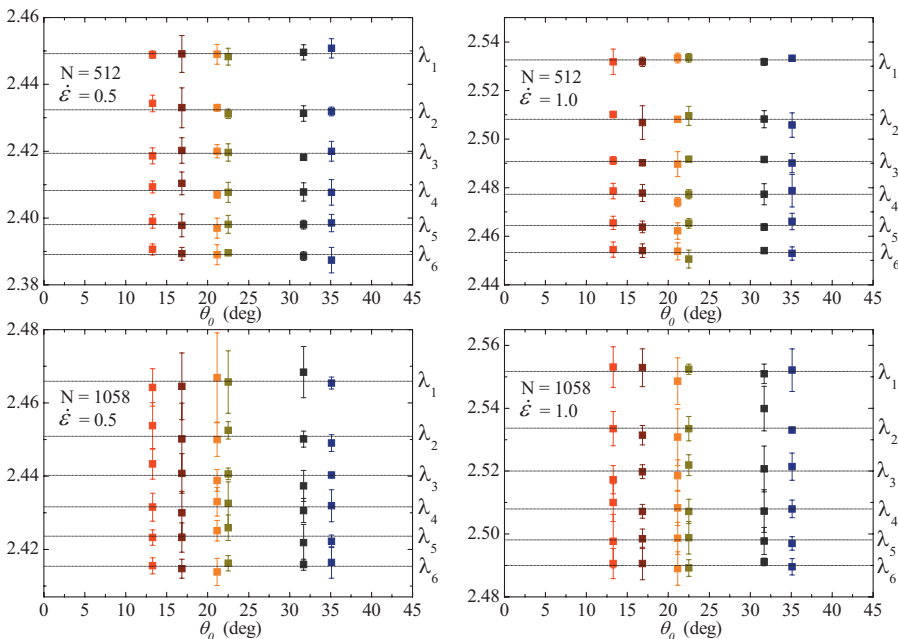

FIG. 2. (Color online) Values of the first six positive Lyapunov exponents for $N = 512$ and $N = 1058$, according to the initial angle of rotation given by conditions 1–6 in Table I. λ_1 is the maximum exponent, λ_2 is the second highest, and so on.
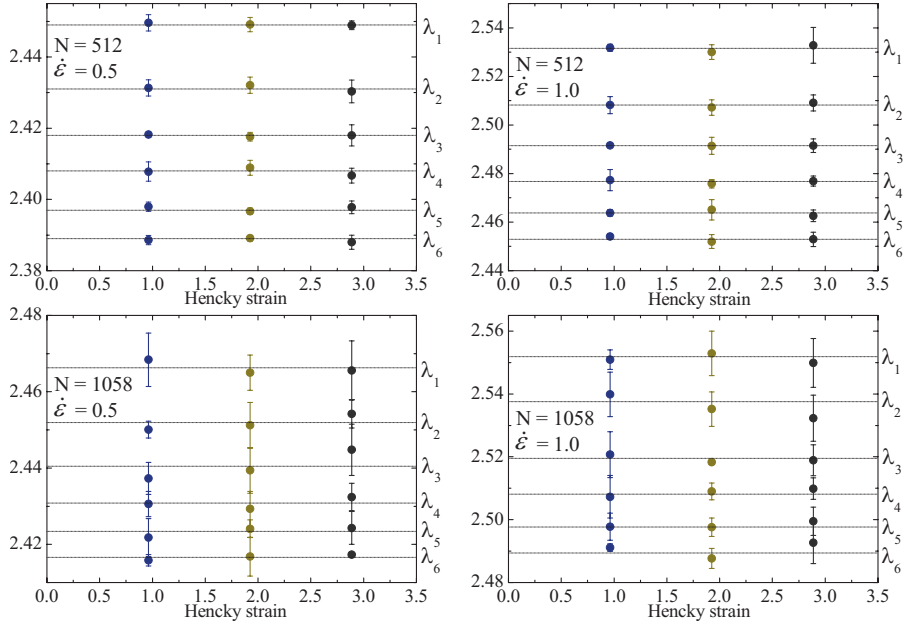
FIG. 3. (Color online) Values of the first six positive Lyapunov exponents for $N=512$ and $N=1058$, with the unit cell initially rotated at an angle $\theta_0=31.72$ (deg) and subject to different Hencky strains according to conditions 5, 7, and 8 in Table I.

To rule out any other possible angle-related effect, conditions with the same Hencky strain and different angles are also compared. In Fig. 4, the differences between exponents in conditions 1–8 and 3–6 of Table I are plotted and labeled by the common ε_P. Between each of the exponents for the two couples of conditions the differences are clearly zero.

From these results we conclude that the independence for systems with large numbers of particles from KR initial conditions is established for the first six positive exponents.

Using the CPR, which has been shown to be valid in this context [11], the results above hold for *all* the independent exponents in the spectrum, as the sum of each ordered pair has to be the same. On the other hand, the CPR does not apply to the Lyapunov couple associated with the displacements parallel to the direction of the flow of Eq. (2) and orthogonal to the temperature surface, as explained in Ref. [11].

We now describe this particular couple in more detail, as the first exponent is especially interesting for our problem. In fact, this is generally referred to as the "unpaired exponent" and, in some nonequilibrium systems with an isokinetic thermostat, it has been found to have a value close to minus the time average of the thermostat multiplier α [1,2]. Departure of this exponent from zero is due to the nonautonomous nature of the dynamics [1] and, in our case, the dynamics is nonautonomous due to the time-dependent boundary conditions. If such boundary conditions were unnecessary, the nonequilibrium system would be autonomous, no periodic remapping of the particles that escape the unit cell would need to be performed and the unpaired exponent would be zero.

There are two equivalent ways to explain this. First and from a dynamical point of view, if the system is autonomous, two points in the phase space do not separate exponentially if
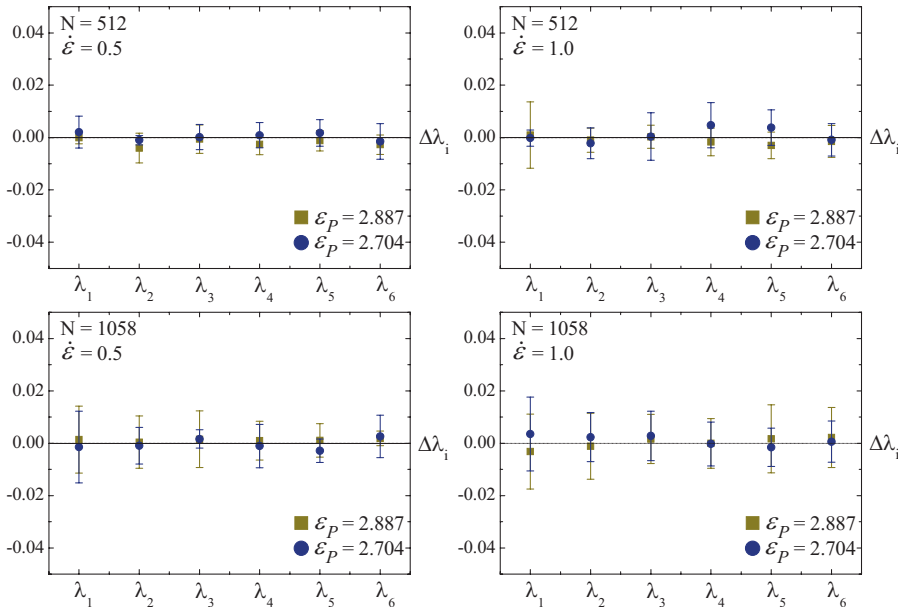

FIG. 4. (Color online) Differences between the first six positive Lyapunov exponents for $N=512$ and $N=1058$ for the coupled conditions 1-8 and 3-6 in Table I. For each couple, the unit cell is initially rotated through different angles θ_0 and subject to the same Hencky strain.

one is chosen along the direction of flow[1] of the other [1,19,20]. Second and from a physical perspective, according to the original proof by Haken [21] in the version discussed in the Appendix of [1], the equations of motion of an autonomous system can be written as $\dot{\boldsymbol{\Gamma}} = \mathbf{G}(\boldsymbol{\Gamma})$. Then $\dot{\boldsymbol{\Gamma}}$ is a tangent vector, because $\ddot{\boldsymbol{\Gamma}} = \frac{\partial \mathbf{G}}{\partial \boldsymbol{\Gamma}} \cdot \dot{\boldsymbol{\Gamma}} = \mathbf{T} \cdot \dot{\boldsymbol{\Gamma}}$, as there is no explicit time dependence in $\mathbf{G}(\boldsymbol{\Gamma})$. The equation for the Lyapunov exponent associated with $\dot{\boldsymbol{\Gamma}}$ can be expressed in a form [1] equivalent to Eq. (4),

$$\lambda = \lim_{t \to \infty} \frac{1}{2t} \ln \frac{|\dot{\boldsymbol{\Gamma}}^2(t)|}{|\dot{\boldsymbol{\Gamma}}^2(0)|},$$

and λ is zero if the numerator is bounded or grows slower than an exponential. Since $\dot{\boldsymbol{\Gamma}}^2(t) = \sum_{i=1}^{N}[\dot{\mathbf{q}}_i^2(t) + \dot{\mathbf{p}}_i^2(t)]$ is a function of the phase variables, its average does not change with time in a steady state (by the definition of a steady state) and the exponent is zero. To sum up, in the PEF Sllod system, it is the periodic remapping that gives rise to a nonzero value and, if a sensitivity to the KR PBCs is present, this exponent should show signs of it.

The second exponent in the unpaired couple maintains a value of zero because an isokinetic constraint is applied to the system. The phase-space trajectories are always on a constant-temperature hypersurface: no deviations in the orthogonal direction are possible.

The size of the systems discussed above is too large to perform a calculation of the full spectrum and of the unpaired exponent. Further insight can be gained with more convenient size and density. Therefore, a second type of system is introduced: a small, dilute, isokinetic eight-particle system with a reduced density $\rho = 0.005$, a reduced temperature $T = 0.7$, and subject to a high elongation rate $\dot{\varepsilon} = 5.0$. The time step chosen is $\Delta t = 5 \times 10^{-6}$ for a total simulation time of $t = 7500$.

At this state point, the force interactions between the particles are extremely weak and the external field component $\dot{\varepsilon}$ is predominant. Any possible contribution coming from the KR PBCs that could be hidden in a denser and less elongated system, due to force-related terms, should be clearly apparent. It is worth noticing that because the isokinetic Gaussian thermostat assumes that the profile of the streaming velocity of the flow $\mathbf{u}$ is linear, no turbulence occurs [3]. Also, it is known that the profile biased thermostat in Eq. (3) causes the appearance of a so-called "string phase" in liquids at high rates [22], where particles travel in strings to minimize the entropy in the system. In our case, given the low density of the sample and the aim of the study, these concerns are irrelevant.

In light of the discussion above, in the low-density system the following approximation for the equations of motion (2) can be used to obtain an estimation of the Lyapunov exponents:

---

[1]The term "flow" in this context is intended in the sense adopted by dynamical systems theory and is not to be mistaken with the flow of mass or energy in the liquid sample.
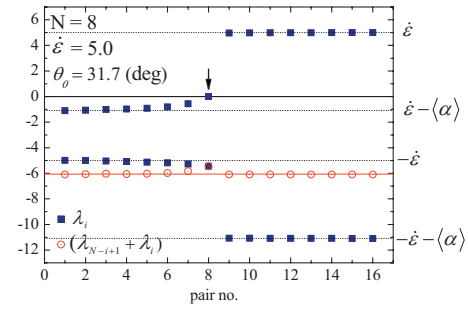

FIG. 5. (Color online) The full spectrum Lyapunov exponents (solid squares) for condition 1 in Table I for a dilute $N=8$ particle system, with a reduced density $\rho = 0.005$ and a reduced temperature $T = 0.7$ and subject to a high elongation rate $\dot{\varepsilon} = 5.0$. The trivial couples associated with the conserved quantities in the system occur at pair No. 1 ($\dot{\varepsilon} - \langle\alpha\rangle$ and $-\dot{\varepsilon}$) and pair No. 15 ($\dot{\varepsilon}$ and $-\dot{\varepsilon} - \langle\alpha\rangle$). The values of the independent exponents are very close to the trivial exponents (dotted lines), due to the low density of the system [see Eq. (6) and the Appendix]. The unpaired couple is No. 8, and one of these exponents is clearly zero (solid arrow) since the system is coupled to an isokinetic thermostat. The sums of the Lyapunov pairs (open circles) and the average value of the sum of independent exponents (solid line) are also shown. Results for the other conditions of Table I are not reported, but they all agree within statistical uncertainty.

$$\dot{\mathbf{q}}_i = \mathbf{p}_i + \dot{\varepsilon}(\mathbf{i}x_i - \mathbf{j}y_i),$$

$$\dot{\mathbf{p}}_i \simeq -\dot{\varepsilon}(\mathbf{i}p_{xi} - \mathbf{j}p_{yi}) - \alpha\mathbf{p}_i. \qquad (6)$$

This is possible since we can assume that collisions between particles are rare, and hence the Lyapunov exponents are dominated by the divergence of trajectories between collisions. By also assuming that α is constant, the Lyapunov exponents associated with initial displacements in the x_i, y_i, p_{xi}, and p_{yi} directions can be determined analytically, and for each particle a set of values $\dot{\varepsilon}$, $-\dot{\varepsilon}$, $\dot{\varepsilon} - \langle\alpha\rangle$, and $-\dot{\varepsilon} - \langle\alpha\rangle$ is found (see the Appendix for the proof). In our system, $(2dN - 2)$ of the exponents can be determined in this manner. The fact that α is not constant and the system is constrained to the constant-temperature hypersurface means that not all particles act independently, and this results in two exponents (the unpaired couple) that cannot be approximated by Eqs. (6).

If any effect due to the KR PBCs is present, a relevant correction to the expected values will be seen in the independent exponents, a PBCs-dependent contribution will appear in the unpaired exponent, or a combination of both will emerge. We first look at the independent exponents and then carry out a separate analysis of the unpaired exponent.

In Fig. 5, the full spectrum of the 32 Lyapunov exponents is shown for condition 1 of Table I. The exponents take on values close to $\dot{\varepsilon}$, $-\dot{\varepsilon}$, $\dot{\varepsilon} - \langle\alpha\rangle$, and $-\dot{\varepsilon} - \langle\alpha\rangle$ as indicated. Incidentally, these values are also the ones associated with the conserved quantities of the system, or the trivial exponents [11], that come from the displacements in the direction of the centre of mass and the total momentum.

TABLE II. Unpaired Lyapunov exponents for the dilute eight-particle system under an elongation rate $\dot{\varepsilon}=5.0$. Initial conditions are numbered according to Table I. λ_{up} is the unpaired Lyapunov exponent, $\langle\alpha\rangle$ is the time average of the thermostat multiplier, and $-\langle\alpha\rangle/\lambda_{up}$ is the ratio between minus the time average of the thermostat multiplier and the exponent. Uncertainties are expressed as twice the standard error of the mean of three independent runs and are next to each relevant quantity.

Initial condition	λ_{up}	2σ	$\langle\alpha\rangle$	2σ	$-\langle\alpha\rangle/\lambda_{up}$	2σ
1	−5.51	0.14	6.15	0.14	−1.12	0.05
2	−5.45	0.07	6.11	0.11	−1.12	0.03
3	−5.46	0.09	6.11	0.07	−1.12	0.03
4	−5.42	0.05	6.04	0.07	−1.12	0.02
5	−5.41	0.03	6.03	0.07	−1.11	0.02
6	−5.46	0.04	6.13	0.04	−1.12	0.02
7	−5.42	0.06	6.05	0.08	−1.11	0.03
8	−5.46	0.07	6.09	0.07	−1.11	0.03

We notice that the small deviations from CPR in the middle of the spectrum in Fig. 5 are due to the fluctuations in the constraint multiplier α, which are of order $O(1/N)$ and have been observed before in systems of small size [1,2,11]. Some contribution due to rare interactions may also cause these results to deviate from those approximated above. The generally good agreement with the expected values and with the CPR indicates that there is no apparent influence of the KR PBCs on the spectrum of Lyapunov exponents.

To confirm our result, we carry out calculations of the spectra for all the other conditions in Table I in search of any possible dependence on $(\theta_0, \varepsilon_P, \tau_P)$. This can be done because the system is at very low density. We find—without explicitly reporting the data for reasons of space—that *all* the independent exponents are within each others' uncertainties for *all* the conditions in Table I and conclude that they are unaffected by the KR PBCs.

The value of the unpaired Lyapunov exponent is shown in Table II. λ_{up} does not display any sensitivity to the initial parameters and has a very similar absolute value to the thermostat multiplier. No correlation of λ_{up} or $\langle\alpha\rangle$ with the initial angle or the Hencky strain is observed, with results obtained

with different initial conditions agreeing within statistical uncertainties.

From Table II it is apparent that the ratio between $\langle\alpha\rangle$ and the unpaired exponent is constant, and close to unity, for each configuration, indicating that λ_{up} is strongly related to the thermal dissipation in the system. Interestingly, $-\langle\alpha\rangle/\lambda_{up}$ appears to be almost independent of the state point, given the same N, for the systems studied. In fact, data of the simulations reported in [11], where two systems with $N=8$ and $N=32$ particles at reduced density $\rho=0.3$, reduced temperature $T=1.0$, and rates $\dot{\varepsilon}=0.5$ and $\dot{\varepsilon}=1.0$ were simulated under condition 1 of Table I, are collated in Table III. Further simulations for $N=32$ and $\dot{\varepsilon}=2.0$ not included in the cited reference are also reported. The ratio $-\langle\alpha\rangle/\lambda_{up}$ for those systems is very close to those for the dilute, strongly elongated system reported in Table II. This is another sign that λ_{up} is not related to the initial conditions of the unit lattice or the way it is remapped: $-\langle\alpha\rangle/\lambda_{up}$ is a property of the sample, depending on N and $\dot{\varepsilon}$, as Table III confirms, and does not bear any relation with the KR PBCs.

The fact that $-\langle\alpha\rangle/\lambda_{up}\approx 1$ can be explained by considering the phase-space contraction of the system under study and recalling that it satisfies the CPR. The average phase-space contraction factor $\langle\Lambda\rangle$ for PEF with an isokinetic Gaussian thermostat is given by [11]

$$\langle\Lambda\rangle = \sum_{i=1}^{2dN}\lambda_i = -\langle\alpha\rangle(dN-1) + \dot{\varepsilon}\left\langle\frac{\displaystyle\sum_{i=1}^{N}(p_{xi}^2-p_{yi}^2)}{\displaystyle\sum_{i=1}^{N}\mathbf{p}_i\cdot\mathbf{p}_i}\right\rangle. \quad (7)$$

We note that in the low-density limit ($\mathbf{F}_i\approx\mathbf{0}$), the final term on the right-hand side of Eq. (7) is equal to the average value of $-\langle\alpha\rangle$ [see Eq. (3)]. Given that in this limit the sum of the $(2dN-2)$ exponents will be approximately $-\langle\alpha\rangle(dN-1)$ as discussed above, the sum of the unpaired exponent and the exponent associated with displacement orthogonal to the constant temperature surface will therefore be equal to $-\langle\alpha\rangle$. Since the exponent associated with displacement orthogonal to the constant-temperature surface is equal to zero in a thermostatted system, this means $\lambda_{up}=-\langle\alpha\rangle$. At higher

TABLE III. Unpaired Lyapunov exponents for the $N=8$ and $N=32$ particle systems reported in [11]. The system has a reduced density $\rho=0.3$ and a reduced temperature $T=1.0$ and is subject to elongation rates $\dot{\varepsilon}=0.5$, $\dot{\varepsilon}=1.0$, and $\dot{\varepsilon}=2.0$ (not included in [11]). "CPR" is the average of the sum of the independent Lyapunov pairs and tends to $-\langle\alpha\rangle$ in the thermodynamic limit. The value of the ratio $-\langle\alpha\rangle/\lambda_{up}$ is almost independent of the state point, as a comparison of these results with those of Table II shows. Also, $-\langle\alpha\rangle/\lambda_{up}$ approaches unity in the thermodynamic limit.

N	$\dot{\varepsilon}$	λ_{up}	2σ	$\langle\alpha\rangle$	2σ	$-\langle\alpha\rangle/\lambda_{up}$	2σ	CPR	2σ
8	0.5	−0.409	0.002	0.442	0.001	1.081	0.008	−0.428	0.005
8	1.0	−1.233	0.002	1.360	0.003	1.103	0.004	−1.314	0.006
32	0.5	−0.415	0.002	0.430	0.001	1.036	0.007	−0.427	0.006
32	1.0	−1.197	0.004	1.259	0.001	1.052	0.004	−1.248	0.006
32	2.0	−3.594	0.002	3.902	0.004	1.086	0.002	−3.847	0.006

TABLE IV. Results for the elongational viscosity for $N=512$ and $N=1058$ at $\rho=0.4$ and reduced temperature $T=1.0$, according to different initial conditions in Table I and different elongation rates. Viscosity data for the dilute small-N system are not reported, but they all agree within statistical uncertainty.

| | $N=512$ | | | | $N=1058$ | | | |
| | $\dot{\varepsilon}=0.5$ | | $\dot{\varepsilon}=1.0$ | | $\dot{\varepsilon}=0.5$ | | $\dot{\varepsilon}=1.0$ | |
Initial condition	η	2σ	η	2σ	η	2σ	η	2σ
1	0.3644	0.0003	0.2849	0.0002	0.3648	0.0008	0.2851	0.0006
2	0.3644	0.0001	0.2847	0.0001	0.3650	0.0003	0.2855	0.0003
3	0.3643	0.0003	0.2849	0.0002	0.3648	0.0001	0.2852	0.0001
4	0.3643	0.0008	0.2850	0.0002	0.3648	0.0004	0.2853	0.0001
5	0.3642	0.0002	0.2850	0.0001	0.3647	0.0007	0.2853	0.0003
6	0.3644	0.0003	0.2850	0.0001	0.3646	0.0004	0.2852	0.0002
7	0.3645	0.0006	0.2849	0.0002	0.3652	0.0003	0.2853	0.0004
8	0.3643	0.0003	0.2849	0.0002	0.3642	0.0009	0.2852	0.0004

densities, we can argue that the CPR predicts that each pair of exponents will sum to $-\langle\alpha\rangle$ with $O(1/N)$ corrections. If these corrections were evenly distributed across the spectrum, this would also explain the result $\lambda_{up}=-\langle\alpha\rangle+O(1/N)$ and is consistent with the observation that the departure of $-\langle\alpha\rangle/\lambda_{up}$ from unity decreases with N. It would be interesting to see if this remains valid at higher densities that those that have been reported in Table I or II. However, this is problematic as there is a maximum density than can be investigated for each system size, and this maximum decreases with a decrease in N, whereas simulations of the full Lyapunov spectrum only become feasible at small N.

III. CONCLUSIONS

It has first been shown that for small and large N the independent exponents are not affected by the initial conditions for $(\theta_0, \varepsilon_P, \tau_P)$. Our numerical results demonstrate that, for small N, the unpaired exponent is also independent of the initial conditions, and it has been argued that this will remain true at large N, where a numerical proof is computationally prohibitive. Finally, tests of Eq. (7) confirm that no effect of KR PBCs is seen on the dynamics of PEF, because Eq. (7) holds independently of any initial value for the KR PBCs. Therefore, we have presented evidence that different implementations of the KR PBCs do not lead to different rates of phase-space separation for the trajectories of systems under PEF and do not have any effect on their dynamics.

As is well known, a formal link between Lyapunov exponents and transport coefficients has been established [1,4,5]. In general, the entropy production rate of a steady-state system is proportional to the sum of the Lyapunov exponents—i.e., $\dot{S}=-k_B\Sigma_{i=1}^{2dN}\lambda_i$—and it can also be expressed as a product of a thermodynamic flux and force—i.e., $\dot{S}=-V\mathbf{J}(\mathbf{F}_e)\cdot\mathbf{F}_e/T$, where V is the volume of the system and the dissipative flux $\mathbf{J}(\mathbf{F}_e)$ is defined in terms of the adiabatic time derivative of the internal energy, or $\dot{H}_0=-V\mathbf{J}(\mathbf{F}_e)\cdot\mathbf{F}_e$ [3].

A transport coefficient $L(\mathbf{F}_e)$ is *defined* as $\mathbf{J}(\mathbf{F}_e)=-L(\mathbf{F}_e)\mathbf{F}_e$, so, for instance, for the viscosity of a system

under PEF, neglecting terms of order $O(1/N)$, we have the relation

$$\eta=-\frac{k_B\langle T\rangle}{4\dot{\varepsilon}^2V}\sum_{i=1}^{2dN}\lambda_i. \qquad (8)$$

Having shown that no contribution from the KR PBCs is present in the spectrum, transport coefficients under different implementations of the PBCs *must* therefore also be the same.

This is confirmed by the results reported in Table IV, where the elongational viscosity for the large-N systems is calculated according to its definition:

$$\eta=-\frac{\langle P_{xx}\rangle-\langle P_{yy}\rangle}{4\dot{\varepsilon}}, \qquad (9)$$

where the angular brackets denote a time average and P_{xx} and P_{yy} are the diagonal components of the instantaneous pressure tensor [3]. From these results, it is evident that there are no reasons for preferring a set of $(\theta_0, \varepsilon_P, \tau_P)$ for KR PBCs over the others, as they all lead to the same viscosity value, within statistical uncertainty. This clearly ensures the integrity of homogeneity in the simulation, confirming the robustness and reliability of the algorithm.

ACKNOWLEDGMENT

APPENDIX

We present a simple analytical proof of the fact that, in the low-density regime, the independent Lyapunov exponents can be approximated by $\dot{\varepsilon}$, $-\dot{\varepsilon}$, $\dot{\varepsilon}-\langle\alpha\rangle$, and $-\dot{\varepsilon}-\langle\alpha\rangle$. Consider the equations of motion (6) for the dilute system,

$$\dot{\mathbf{q}}_i=\mathbf{p}_i+\dot{\varepsilon}(\mathbf{i}x_i-\mathbf{j}y_i),$$

$$\dot{\mathbf{p}}_i = -\dot{\varepsilon}(\mathbf{i}p_{xi} - \mathbf{j}p_{yi}) - \alpha\mathbf{p}_i,$$

and assume that the thermostat multiplier α is constant. The equations of motion for the particles are then independent and each particle can be considered separately. From now on, we drop the subscript i that refers to the particle.

The equations of motion for the components of the tangent vector $\delta\Gamma$ become

$$\delta\dot{x} = \delta p_x + \dot{\varepsilon}\delta x, \tag{A1}$$

$$\delta\dot{y} = \delta p_y - \dot{\varepsilon}\delta y, \tag{A2}$$

$$\delta\dot{p}_x = -(\dot{\varepsilon} + \alpha)\delta p_x, \tag{A3}$$

$$\delta\dot{p}_y = (\dot{\varepsilon} - \alpha)\delta p_y. \tag{A4}$$

Equations (A3) and (A4) can be solved to give

$$\delta p_x(t) = e^{-(\dot{\varepsilon}+\alpha)t}\delta p_x(0), \tag{A5}$$

$$\delta p_y(t) = e^{(\dot{\varepsilon}-\alpha)t}\delta p_y(0), \tag{A6}$$

where $\delta p_x(0)$ and $\delta p_y(0)$ are the initial displacement at time $t=0$ in x and y directions of the momentum, respectively. Then, these can be substituted into Eqs. (A1) and (A2) to give

$$\delta\dot{x}(t) = e^{-(\dot{\varepsilon}+\alpha)t}\delta p_x(0) + \dot{\varepsilon}\delta x(t), \tag{A7}$$

$$\delta\dot{y}(t) = e^{(\dot{\varepsilon}-\alpha)t}\delta p_y(0) - \dot{\varepsilon}\delta y(t), \tag{A8}$$

and these can be solved to give

$$\delta x(t) = -\frac{\delta p_x(0)}{2\dot{\varepsilon}+\alpha}(e^{-(\dot{\varepsilon}+\alpha)t} - e^{\dot{\varepsilon}t}) + \delta x(0)e^{\dot{\varepsilon}t}, \tag{A9}$$

$$\delta y(t) = \frac{\delta p_y(0)}{2\dot{\varepsilon}+\alpha}(e^{(\dot{\varepsilon}-\alpha)t} - e^{-\dot{\varepsilon}t}) + \delta y(0)e^{-\dot{\varepsilon}t}. \tag{A10}$$

A suitable choice of an orthonormal basis of initial vectors [18] is represented by the vectors with independent displacements along the x, y, p_x, and p_y directions, so that, omitting the normalization parameters, we can write

$$\delta\Gamma_x(0) = (\delta x(0), 0, 0, 0),$$

$$\delta\Gamma_y(0) = (0, \delta y(0), 0, 0),$$

$$\delta\Gamma_{p_x}(0) = (0, 0, \delta p_x(0), 0),$$

$$\delta\Gamma_{p_y}(0) = (0, 0, 0, \delta p_y(0)).$$

Consider the first vector, when the initial displacement in the x direction is $\delta x(0)=a$, where a is small (in numerical simulations and in reduced units $a=0.0001$, according to the second reference in [2]) and all other initial displacements along y, p_x, and p_y are zero. $\delta x(0)$ will grow exponentially in time according to Eq. (A9), with a rate $\dot{\varepsilon}$. Clearly, all other components will remain zero according to Eqs. (A5), (A6), and (A10), so that the exponent associated with $\delta\Gamma_x$ will have a value $\dot{\varepsilon}$.

A similar argument can be used for $\delta\Gamma_y$: if $\delta y(0)=a$, it will grow exponentially in time with a rate $-\dot{\varepsilon}$. Again, all other initial displacements along x, p_x, and p_y are zero, so they will remain zero. The associated Lyapunov exponent will therefore have a value $-\dot{\varepsilon}$.

The case for $\delta\Gamma_{p_x}$ is different: if $\delta p_x(0)=a$, this component will grow exponentially with a rate $-(\dot{\varepsilon}+\alpha)$. The components in the y and p_y directions remain zero, but the x component will grow exponentially with a rate $\dot{\varepsilon}$, according to the dominant exponent in the first term of Eq. (A9). But the only nonzero component of the resultant vector, which must remain orthogonal to $\delta\Gamma_x$ according to [18], will grow exponentially with the rate $-(\dot{\varepsilon}+\alpha)$, and therefore there is a Lyapunov exponent $-(\dot{\varepsilon}+\alpha)$ associated with $\delta\Gamma_{p_x}$.

Finally, for $\delta\Gamma_{p_y}$, if $\delta p_y(0)=a$, this component will grow exponentially with a rate $\dot{\varepsilon}-\alpha$. The components in the x and p_x directions remain zero, but δy will grow exponentially with a rate either $-\dot{\varepsilon}$ or $\dot{\varepsilon}-\alpha$ because of Eq. (A10), depending on which one is larger. As above, the only nonzero component of the resultant vector, which again has to be orthogonal to $\delta\Gamma_y$, will grow exponentially with the rate $\dot{\varepsilon}-\alpha$ and there is a corresponding Lyapunov exponent with this value.

The values $\dot{\varepsilon}$, $-\dot{\varepsilon}$, $\dot{\varepsilon}-\langle\alpha\rangle$, and $-\dot{\varepsilon}-\langle\alpha\rangle$ for the independent exponents in the dilute regime are obtained from the above arguments, approximating α with its time average $\langle\alpha\rangle$.

[1] S. Sarman, D. J. Evans, and G. P. Morriss, Phys. Rev. A **45**, 2233 (1992).

[2] Some of the most interesting results can also be found in the following: G. P. Morriss, Phys. Lett. A **134**, 307 (1989); Phys. Rev. A **37**, 2118 (1988); H. A. Posch and W. G. Hoover, *ibid.* **39**, 2175 (1989); D. J. Evans, E. G. D. Cohen, and G. P. Morriss, *ibid.* **42**, 5990 (1990); D. J. Searles, D. J. Evans, and D. J. Isbister, Chaos **8**, 337 (1998); G. P. Morriss, Phys. Rev. E **65**, 017201 (2001).

[3] D. J. Evans and G. P. Morriss, *Statistical Mechanics of Nonequilibrium Liquids* (Academic, New York, 1990); S. S. Sarman, D. J. Evans, and P. T. Cummings, Phys. Rep. **305**, 1

(1998).

[4] H. A. Posch and W. G. Hoover, Phys. Rev. A **38**, 473 (1988).

[5] E. G. D. Cohen, Physica A **213**, 293 (1994).

[6] A partial collection of works is given by the following: Ch. Dellago, H. A. Posch, and W. G. Hoover, Phys. Rev. E **53**, 1485 (1996); J. P. Eckmann and O. Gat, J. Stat. Phys. **98**, 775 (2000); S. McNamara and M. Mareschal, Phys. Rev. E **64**, 051103 (2001); W. G. Hoover *et al.*, J. Stat. Phys. **109**, 765 (2002); T. Taniguchi and G. P. Morriss, Phys. Rev. E **65**, 056202 (2002); **68**, 026218 (2003); **68**, 046203 (2003); Phys. Rev. Lett. **94**, 154101 (2005); Phys. Rev. E **71**, 016218 (2005); T. Taniguchi, C. Dettmann, and G. P. Morriss, J. Stat.

Phys. **109**, 747 (2004).

[7] B. D. Todd and P. J. Daivis, Phys. Rev. Lett. **81**, 1118 (1998); P. J. Daivis and B. D. Todd, J. Chem. Phys. **124**, 194103 (2006).

[8] A. M. Kraynik and D. A. Reinelt, Int. J. Multiphase Flow **18**, 1045 (1992).

[9] V. I. Arnold and A. Avez, *Ergodic Problems of Classical Mechanics* (Benjamin, New York, 1968).

[10] T. A. Hunt and B. D. Todd, Mol. Phys. **101**, 3445 (2003).

[11] F. Frascoli, D. J. Searles, and B. D. Todd, Phys. Rev. E **73**, 046206 (2006).

[12] J. C. Sprott, *Chaos and Time-Series Analysis* (Oxford University Press, New York, 2003).

[13] B. D. Todd and P. J. Daivis, Comput. Phys. Commun. **117**, 191 (1999).

[14] A. Baranyai and P. T. Cummings, J. Chem. Phys. **110**, 42

(1999).

[15] J. D. Weeks, D. Chandler, and H. C. Andersen, J. Chem. Phys. **54**, 5237 (1985).

[16] J. Petravic and D. J. Evans, Mol. Phys. **95**, 219 (1998).

[17] B. D. Todd and P. J. Daivis, J. Chem. Phys., **112**, 40 (2000).

[18] G. Benettin, L. Galgani, and J. M. Strelcyn, Phys. Rev. A **14**, 2338 (1976); G. Benettin, L. Galgani, A. Giorgilli, and J.-M. Strelcyn, Meccanica **15**, 9 (1980); **15**, 21 (1980); I. Shimada and T. Nagashima, Prog. Theor. Phys. **61**, 1605 (1979).

[19] C. P. Dettmann and G. P. Morriss, Phys. Rev. E **53**, R5545 (1996).

[20] D. Panja and R. van Zon, Phys. Rev. E **66**, 021101 (2002).

[21] H. Haken, Phys. Lett. **94A**, 71 (1983).

[22] D. J. Evans and G. P. Morriss, Phys. Rev. Lett. **56**, 2172 (1986).